IUTAM Symposium on 50 Years of Chaos : Applied and Theoretical
Kyoto, Japan, November 28 - December 2, 2011

Analysis of ILM Logic Operations via van der Pol Phase Planes

M. Sato [1], N. Fujita [1], S. Imai [1], S. Nishimura [1], W. Shi[1], Y. Soga [1] and A. J. Sievers [2]
[1] *Graduate School of Natural Science and Technology, Kanazawa University, Kanazawa, Japan, msato@kenroku.kanazawa-u.ac.jp*
[2] *Laboratory of Atomic and Solid State Physics, Cornell University, Ithaca NY, USA*

Logic operations that have previously been numerically demonstrated for intrinsic localized modes (ILMs) in a driven nonlinear lattice are analyzed using van der Pol phase planes. The time dependent application of a vibrational impurity mode at the lattice site of interest either can produce or destroy an incipient ILM that is the input. The appearance or absence of the resulting ILM can be understood via paths in the phase plane controlled by the evolving attractors associated with the time dependent impurity mode.

Introduction

Micro-electro mechanical systems (MEMS) now have a variety of applications. With the continuing decrease in size the nonlinear vibrational properties of such MEMS resonators can no longer be ignored. We have studied driven MEMS nonlinear lattices and found a nonlinear localized excitation called an intrinsic localized mode (ILM).[1] Driver locked ILMs are self sustained localized oscillations and are stationary stable. This feature makes them attractive for information processing.

Previously we have demonstrated logic operations based on ILM-impurity interactions by means of numerical simulations.[2] Logic "1" or "0" is coded with the existence or absence of the ILM. The lattice is a micro-cantilever array, and the sign of the nearest-neighbour nonlinearity is positive. Linear mode analysis presents a band of normal mode frequencies. Because of the positive sign of the nonlinearity, an ILM can be generated above this frequency band, maximum frequency ω_m, and appear in the form of dynamical localized excitation with frequency ω_0. To produce an ILM at a specific lattice location and specific frequency the driver is set to the desired frequency and a lattice defect is introduced at that site in the array so that it produces a linear defect mode above the top of the band. The strength of the defect is increased with time until the corresponding impurity mode frequency coincides with the driver frequency. The resultant signal is an amplitude modulated cantilever vibration because of the transient response. Next the impurity is removed from the lattice by decreasing its strength. Depending on the relative phase of the amplitude modulation at the time when the impurity mode strength is decreased either an ILM is generated or no ILM appears in the perfect lattice.

Analysis and Discussion

Although it may appear that this nonlinear system involves many degrees of freedom an ILM spans only a few lattice sites; in addition, the amplitude of the driver locked vibration is determined by the driver frequency as for a single Duffing oscillator. Thus, we introduce here the van der Pol phase plane as an analysis tool, although it is usually used to describe a single resonator. The ILM center motion is decomposed into $a(t)\cos\Omega t + b(t)\sin\Omega t$ using the cosine driver at frequency Ω as a reference. Because the simulation model includes both the driver and damping, the system has attractor(s). A novel feature of this presentation scheme is that since the strength of the impurity mode changes with time the attractor(s) will move with time.

Figure 1 displays the entire van der Pol phase paths for (a) ILM development and (b) no-ILM result when the impurity mode frequency is varied from $\omega_0/\omega_m = 1.00 \rightarrow 1.013 \rightarrow 1.00$. The solid and dashed curves in (a) and (b) are the trajectories for the ILM and no-ILM cases, respectively. In both frames, the paths start from the origin, and spiral around the impurity mode attractor; however, depending on the relative phase of the amplitude modulation at the time when the impurity mode strength is decreased (a) shows the change into the large amplitude ILM while (b) does not.

To better understand this switching process we now examine the last part of the two paths where $\omega_0/\omega_m = 1.013 \rightarrow 1.00$ since the end result strongly depends on the removal timing relative to the phase of the AM modulation. These van der Pol plots are shown in Fig. 2. With the impurity mode at full strength the AM modulated impurity mode path is given by the solid curve in Fig. 2(a), starting at the bottom of the figure and circling around the fixed attractor center, identified by the triangle. At the open circle position the strength of the impurity mode begins to decrease and the resultant path for this no-ILM is represented by the dashed curve that peels off to the left, away from that particular attractor. The time dependence of the center

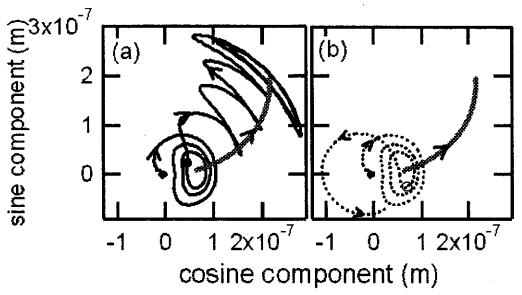

Figure 1:(a) Complete van der Pol phase path for the generation of the large amplitude ILM when the impurity mode frequency is varied from $\omega_0/\omega_m = 1.00 \rightarrow 1.013 \rightarrow 1.00$. The initial spiral path is that of the driven impurity mode. (b) The dashed curve represents the corresponding path for the trajectory in the no-ILM case. See text for details. The thick arc in (a,b) shows the time dependent attractor for the ILM.

of the no-ILM attractor is identified in the figure. If, on the other hand, the strength of the impurity mode begins to decrease at a later time, represented by the solid dot then the path peels off to the right, moving in the same direction as that time dependent ILM attractor as shown. To follow the paths relative to the attractors, their basins are calculated for three different impurity mode frequencies, the maximum frequency plus two smaller values: $\omega_0/\omega_m = 1.013,\ 1.011,\ 1.010$. Figure 2(b,c,d) are for the ILM case. The solid dot represents the ILM path position for that particular local mode frequency and the open circles in Fig. 2(e,f,g) represent the no-ILM positions for the same local mode frequencies. In each case the path just follows the spiral orbit towards its attractor located at that particular time (local mode frequency). Another interesting feature is the appearance of two attractors as the local mode frequency decreases. This illustrates how the impurity mode changes to an impurity-trapped ILM. Finally compare the solid and open circles of Fig. 2(c,f) with those in Fig. 2(d,g). Initially, both trajectories are in the same basin of the high amplitude trapped-ILM state. However, at $\omega_0/\omega_m = 1.010$, the solid circle remains in the same basin while the open circle is in another basin of the lower amplitude (no ILM) state.

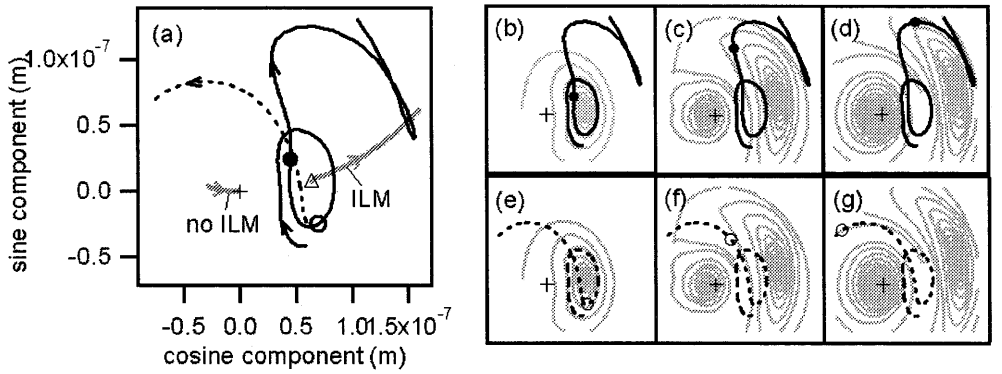

Figure2: (a)Trajectories of the ILM and the no ILM for the initial decent of the impurity mode frequency. Origin is marked by "+". The open circle indicates the initial decent time for the no ILM case (dotted curve). The solid dot indicates the corresponding time for the ILM case. The one attractor located at the triangle position evolves into the final two attractors shown in gray. Fig. 2(b-g) Evolution of the attractor basins with changing impurity mode frequency (gray spirals). Frames (b,c,d): Each solid circle is a point on the trajectory of the solid curve in Fig. 2(a) at impurity mode frequency $\omega_0/\omega_m = 1.013,\ 1.011,\ 1.010$, respectively. These solid circles are superimposed on the spiral orbit basins leading toward the attractor(s) for the same impurity mode frequencies. Frames (e,f,g): The same development, using open circles for the same three moments, is shown for the no-ILM dashed curve in Fig. 2(a).

Conclusions

Logic operations are analyzed using van der Pol phase planes. The trajectory in the phase plane of a driven ILM are explained by the motion of attractors that are controlled by application of a time-depended impurity mode. If the initial decent in impurity mode frequency, after seeding the ILM, is positioned in the upper half of the van der Pol spiral path around the attractor, a large amplitude ILM can be formed; while, if it is positioned in the lower half no ILM results.

References

[1] M. Sato, B. E. Hubbard, and A. J. Sievers, Nonlinear energy localization and its manipulation in micromechanical oscillator arrays, Rev. Mod. Phys., vol. **70**, pp. 137-157, 2006.

[2] M. Sato, N. Fujita and A. J. Sievers, Logic operations demonstrated with localized vibrations in a micromechanical cantilever array, to be published in DCDS-S, vol. **4**, No.5, 2011. arXiv:1001.4286v1